A Sparse Multistatic Imaging System for Terahertz Volume Inspection

B. Baccouche[1], M. Kahl[2], A. Keil[3], P. Haring Bolivar[2], T. Loeffler[4], J. Jonuscheit[1], and F. Friederich[1]
[1]Fraunhofer Institute for Physical Measurement Techniques IPM, 67663 Kaiserslautern, Germany
[2]University Siegen, High Frequency and Quantum Electronics, 57076 Siegen, Germany
[3]Becker Photonik GmbH, 32457 Porta Westfalica, Germany
[4]Synview GmbH, 61348 Bad Homburg, Germany

***Abstract*—Frequency modulated terahertz imaging systems have shown a great potential for volume inspections in the industrial process and quality control. However, many system concepts lack the capability to encompass a large field of view with fast data acquisition speed, while providing significant depth information. Based on our recently outlined system design of a terahertz imaging solution for the industrial process control, we report on the realization of a stepped-frequency modulated sparse array with 12 emitters and 12 heterodyne receivers operating in the frequency range from 75 GHz to 110 GHz. The system is ready to perform imaging tasks and will be in a final step combined with a band-conveyor for fast terahertz image acquisition.**

I. INTRODUCTION

TERAHERTZ imaging systems have proven to be highly desirable for non-destructive testing tasks. Especially frequency modulated continuous-wave imaging systems operating in the sub-terahertz regime have shown a great potential for volume inspections in industrial applications [1]. Nevertheless, the usage of this technology in an industrial production environment places high demands on image acquisition speed, scalability, cost-effectiveness and detection sensitivity. In the last years several interesting approaches for terahertz imaging systems with real-time capabilities were introduced [2]. In most cases these concepts are based on either full sensor arrays or fast scanning optics. Quasi-optical systems suffer from limited lateral resolution within fixed focal distances, while most system concepts with fully populated sensor arrays demand a trade-off between field of view and image resolution because of the limited array size. The usage of sparse arrays in combination with numerical focusing algorithms is an efficient solution that overcomes afore mentioned limitations at the cost of higher computational loads.

In this contribution we report on our realization of a terahertz continuous-wave multistatic sparse array for application in the industrial process control, based on our earlier outlined terahertz system design [3]. The array operates in a frequency range between 75 GHz - 110 GHz and represents a multistatic synthetic aperture radar (SAR) [4]. It consists of 12 transmitters (Tx) and 12 heterodyne receivers (Rx), which are used to spatially sample the test object. The combination with a band-conveyor allows the generation of a synthetic aperture. A stepped-frequency continuous-wave signal modulation of 35 GHz bandwidth provides accurate depth resolution. In order to reduce system complexity and costs while preserving decent image quality, the spatial distribution of the transmitters and receivers is derived from the so called effective aperture approach.

II. SYSTEM SETUP

The realized sparse transceiver array is depicted in Fig. 1. The 12 transmitters are placed in a linear fashion with an equidistant element spacing of 6 cm. The 12 receivers are placed in the array center and divided in two sub-arrays with 6 elements each.

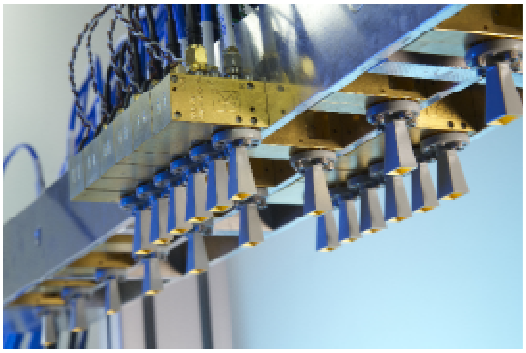

Fig. 1. Realized sparse array containing 12 transmitters and 12 heterodyne receivers.

The elements of a sub-array have an equal spacing of 2 cm. A switching matrix is used to sequentially operate the emitters for each frequency point, while the receivers simultaneously record the received signal from the illuminated object. Reconstruction algorithms base on the matched-filter approach are implemented on a graphics processing unit (GPU).

III. IMAGING USING A SPARSE MULTISTATIC ARRAY

The usage of matched filtering as focusing approach puts constraints on the spacing between the array elements. The upper bound of elements spacing is half of the smallest wavelength. The arising system complexity can be dramatically decreased if the array is designed in a sparse fashion based on the so called effective aperture approach [5]. This implies that the convolution of the transmitter's spatial distribution with the receiver's spatial distribution results in an effective monostatic spatial distribution, which is equivalent to one of a full transceiver array. This way the emitter array can be populated in a sparse fashion of the desired full aperture while the receiver array can be used as an interpolator or vice versa. Assuming a Tx array with N_T elements and a Rx array with N_R elements, the resulting effective aperture will contain $N_T \times N_R$ Transceivers. Due to the physical dimensions of the transmitters and receivers, the minimum achievable elements spacing is 2 cm. Thus the spatial distribution of the elements of the Tx array and the Rx array has to be chosen, so that each array compensates for artifacts from the other. That is, considering the point spread function (PSF) of each array, the minima of an array's PSF have to coincide with the grating

lobes of the other array's PSF and vice versa. Simulated 1-D PSFs of the Tx array, the Rx array and the combination of both are depicted in Fig. 2. Simulation data has been obtained while assuming a point reflector located in front of the array center at a distance of 73 cm.

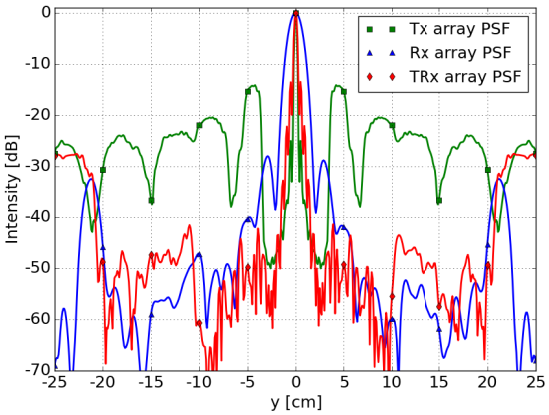

Fig. 2. Tx array PSF, Rx array PSF and whole array PSF.

On one hand the Tx PSF yields a sharp peak at coordinate's origin, yet surrounded with grating lobes that reach -14 dB. On the other hand the Rx PSF yields a broader center peak with minima that coincide with the Tx PSF lobes. As a result the PSF of the combined array yields a sharp peak that agrees with the one of the Tx PSF, while its grating lobes level is below -40 dB within a section of ca. 40 cm. Residual Lobes beyond this section will be suppressed in a next step using adaptive signal processing methods as proposed in [6].

IV. Measurement of the Array's 2-D PSF

The array has to be calibrated before performing measurements. The aim of the calibration procedure is to suppress system and background noise as well as to correct array phase center displacements. A match measurement and an offset-short measurement, using a 100 cm tall metallic cylinder with 6 cm radius are used as calibration data. The cylinder is placed in front of the array center in a distance of 75 cm, while having its axis orthogonal to the array axis. The curvature of the cylinder is involved in the calibration procedure using a numerically determined phase term C_{sim}. Accordingly the corrected measurement M_{cor} of a Tx-Rx combination raw measurement M_{raw} is given by,

$$M_{cor} = \frac{M_{raw} - M_{match}}{M_{short} - M_{match}} \times C_{sim}.$$

In order to compare with previous PSF simulations, we measure the array's 2-D PSF using a 100 cm tall metallic rod of 2.5 mm radius as point reflector. The rod is held in front of the array center at a range of 75 cm while having its axis orthogonal to the array axis. The rod is then sequentially illuminated by a linear sweep of 100 frequency points going from 75 GHz to 110 GHz. Each measurement is averaged 3 times to increase signal-to-noise ratio, resulting in a total acquisition time of ca. 90 ms. Even though the signal acquisition time per Tx and frequency point does not exceed 10 µs, the frequency switching time of ca. 300 µs is still the main limitation of the data acquisition speed. As depicted in Fig. 3, the measured PSF agrees well with the simulated one and yields a Rayleigh range resolution of ca. 4.5 mm and a lateral resolution in y-direction of ca. 4 mm. In the grating lobes free section the image dynamic range of the experimentally determined PSF reaches nearly 40 dB. This is still below the simulated results, because of residual background echoes of the received signal.

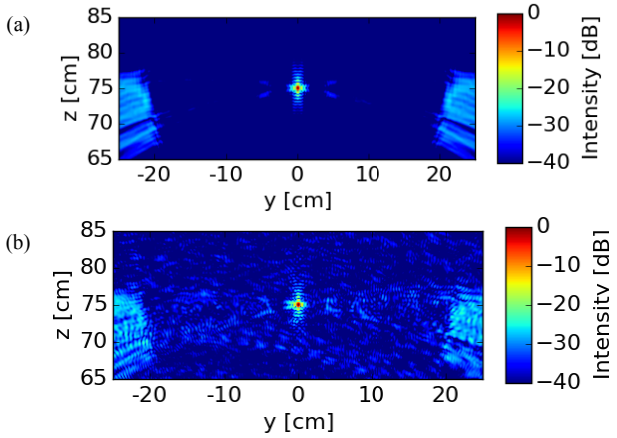

Fig. 3. Normalized intensity 2-D PSF: (a) Simulation, (b) Measurement.

V. Conclusion

A sparse multistatic line array containing 12 emitters and 12 receivers, which operate in the W band, has been realized for imaging applications. Lateral and range resolutions below 5 mm within an image dynamic range of nearly 40 dB are experimentally demonstrated. This imaging quality is achieved with a fraction of sensor elements in comparison with an equivalent full transceiver array. Limited by the frequency switching time, feed motion speeds of the band-conveyor range currently from 5 cm/s to 20 cm/s. Aiming to deliver a volume inspection system for industrial process control, ongoing works are focused on speed and image quality optimization as well as image formation in real time.

Acknowledgment

This work was supported by FhG Internal Programs under Grant No. Attract 018-692 158 and the European Fund for Regional Development (EFRE) under Grant No. 961-52 123/40 (16) 81047970.

References

[1]. E. Cristofani, et al., "Nondestructive testing potential evaluation of a terahertz frequency-modulated continuous-wave imager for composite materials inspection," *Opt. Eng.,* vol. 53(3), 031211, March, 2014.

[2]. F. Friederich, et al., "THz active imaging systems with real-time capabilities," *IEEE Trans. Terahertz Sci. Technol.,* vol. 1(1), pp. 183-200, Sept., 2011.

[3]. F. Friederich, et al., "Towards 3-D volume inspection for process control," *39th International Conference on Infrared, millimeter, and Terahertz waves (IRMMW-THz)*, Sep, 2014.

[4]. M. Soumekh, "Bistatic synthetic aperture radar inversion with application in dynamic object imaging," *IEEE Transactions on Signal Processing*, vol.39, no.9, pp.2044, 2055, Sep, 1991

[5]. G. Lockwood and F. Foster, "Optimizing sparse two-dimensional transducer arrays using an effective aperture approach," *IEEE Ultrasonics Symposium Proceedings*, vol. 3, pp. 1497-1501, Oct, 1994.

[6]. Zhuopeng Zhang and T. Buma, "Terahertz impulse imaging with sparse arrays and adaptive reconstruction," *IEEE Journal of Selected Topics in Quantum Electronics,* vol. 17, pp. 169-176, Jan, 2011.